https://doi.org/10.5194/egusphere-2025-5830
Preprint. Discussion started: 14 January 2026

A Process-Based Four-Stage Framework for Seismic Resilience Assessment of Urban Water Distribution Networks through Multi-Attribute Metrics

Huiquan Miao[a], Ya'nan Liu[a], Benwei Hou[a, *], Jie Wei[b], Chengshun Xu[a]

[a] Key Laboratory of Urban Security and Disaster Engineering, Ministry of Education, Beijing University of Technology, Beijing 100124, China;

[b] Key Laboratory of Structures Dynamic Behavior and Control, Ministry of Education, Harbin Institute of Technology, Harbin 150090, China

Correspondence: Benwei Hou (benweihou@bjut.edu.cn)

Abstract: Urban water distribution networks are critical lifelines whose seismic resilience is essential for maintaining daily functions and post-disaster service continuity. However, most existing studies focus on seismic-induced functional failures and short-term recovery, while neglecting pre-disaster preparedness and long-term adaptation—two stages that fundamentally shape the overall resilience trajectory. Conventional assessments typically rely on single-dimensional hydraulic or network indicators, which tend to be one-sided and error-prone. These limitations hinder a comprehensive understanding of WDN behavior across different seismic disturbance stages, yielding only coarse performance judgments that offer limited guidance for diagnosing vulnerabilities or planning effective resilience enhancement and retrofit strategies. To address these limitations, this study proposes a process-based four-stage seismic resilience framework that explicitly incorporates preparedness, robustness, recoverability, and long-term adaptation, capturing the full evolution of WDN performance during seismic events. A multi-attribute indicator system integrating topological homogeneity, energy redundancy, pipeline fragility, hydraulic service performance, and recovery efficiency is developed to enable refined stage-specific assessment. An adaptation index (ACI) is further introduced to quantify the integrated improvement achieved by different retrofit strategies. Applications to the Jilin and Mianzhu WDNs demonstrate clear stage-dependent resilience disparities and provide actionable guidance for optimizing seismic resilience enhancement. Application to the Jilin and Mianzhu WDNs demonstrates the framework's applicability and reveals clear stage-dependent resilience disparities, which provide scientifically grounded guidance for optimizing seismic resilience enhancement in urban WDNs.

Key Words: Water distribution network; Monte Carlo simulation; Seismic resilience framework; Four-stage assessment; Resilience enhancement strategies

https://doi.org/10.5194/egusphere-2025-5830
Preprint. Discussion started: 14 January 2026

1 Introduction

As a critical lifeline engineering system, urban water distribution networks (WDNs) not only ensure daily domestic water supply but also play an irreplaceable role in post-disaster emergency response, firefighting, and public livelihood support. However, earthquakes frequently cause extensive and severe damage to WDNs. Historical seismic disasters have demonstrated that WDN failure can trigger widespread water supply interruptions and secondary hazards, such as urban fires and public health crises (Bouziou et al., 2017; Takada et al., 1992). For example, the 1906 San Francisco earthquake ruptured more than 300 pipelines and ignited over 60 secondary fires. Due to the lack of firefighting water, the fires burned for three consecutive days, destroying 492 city blocks and killing more than 3,000 people; the losses from secondary fires were three times greater than those caused directly by the earthquake (Scawthorn et al., 2006). In the 1976 Tangshan earthquake, 140 km of pipelines were damaged at 646 locations, leaving residents without water for over a week. The resulting water shortage led to outbreaks of infectious diseases such as dysentery, with household infection rates reaching 89.3% in some areas (Liu et al., 2002). Similarly, the 1995 Kobe earthquake caused nearly 1,000 joint failures and widespread disruption of firefighting water supply, severely impeding fire suppression efforts (Kuraoka et al., 1996). Other serious disasters, such as the Chile, Lushan, and Wenchuan earthquakes (Tang et al., 2013; Eidinger et al., 2014; Tang, 2014), further underscore that enhancing the seismic resilience of WDNs has become a critical priority for urban disaster prevention and mitigation.

The growing emphasis on resilience research has highlighted the need for systematic frameworks to evaluate and enhance infrastructure performance under serious disasters. Bruneau et al. (2003) pioneered the community seismic resilience framework, defining it as "the ability of social units to mitigate hazards, contain disaster impacts, and recover in ways that minimize social disruption and reduce future earthquake effects." They conceptualized resilience across four dimensions—technical, organizational, social, and economic—with attributes of robustness, redundancy, resourcefulness, and rapidity. Building on this foundation, researchers have applied multi-stage, dynamic resilience assessments to diverse lifeline systems (Cimellaro et al., 2016; Shin et al., 2018; Ouyang et al., 2012; Nan et al., 2017). The U.S. National Academy of Sciences (American Lifelines Alliance [ALA], 2005) formalized this approach through a "Preparedness–Absorption–Recovery–Adaptation" cycle, in which infrastructure sequentially passes through four stages to complete a resilience loop. Exemplifying this trend, Xu et al. (2022) proposed a four-stage seismic resilience assessment for metro systems; Zhang et al. (2018) developed a three-stage resilience-oriented decision framework for road networks—pre-disaster mitigation, post-disaster emergency response, and long-term recovery—to guide stochastic multi-objective optimization; and Zong et al. (2022) evaluated gas network resilience through pre-disaster network enhancement, post-disaster pressure testing, and restoration. Also, multi-stage resilience assessment has been extended to healthcare facilities (Pei et al., 2025), power systems (Sun et al., 2019; Xie et al., 2025), and interdependent infrastructure networks (Ravadanegh et al., 2022), demonstrating the framework's versatility and growing relevance in infrastructure risk management.

https://doi.org/10.5194/egusphere-2025-5830
Preprint. Discussion started: 14 January 2026

In the field of water distribution network (WDN) resilience, extensive research has been devoted to developing assessment frameworks and indicator systems (Diao et al., 2016; Cimellaro et al., 2015). Zhang et al. (2024) divided WDN resilience into three stages—pre-disaster preparedness, post-disaster response, and recovery—and established a staged evaluation framework. Chen et al. (2025) incorporated resistance, absorption, and recovery capacities, employing the Sobol sequence-based Quasi-Monte Carlo (QMC) method to assess the seismic resilience of large-scale WDNs. Zhou et al. (2022) further proposed a three-stage dynamic framework to evaluate the comprehensive resilience of rural water supply systems (RWSS) at different stages. Although these studies acknowledge the staged evolution of resilience, most adopt three-stage or lifecycle-based divisions that inadequately capture the dynamic evolution of the entire earthquake process. Fundamental questions—such as how to delineate the seismic resilience stages of WDNs and identify the dominant resilience characteristics within each stage—remain insufficiently explored. Moreover, existing studies lack quantitative methods to characterize the adaptive attribute of resilience, limiting their ability to represent the system's enhanced capacity to cope with subsequent hazards (Zhang et al., 2024).

Four primary methods have been developed for WDN resilience evaluation: indicator-based, energy-based, complex network-based, and recovery simulation methods. (1) The indicator-based method extracts factors reflecting system resilience, scores them, and derives the final assessment. For example, Woolf et al. (2016) used a subjective 1-5 scale to score WDN resilience; Cimellaro et al. (2016) used the proportion of households without tap water; Miao et al. (2021) used indicators like per capita pipeline length and per capita water consumption. While simple to implement, these methods heavily rely on researchers' subjective experience. (2) The energy-based method defines resilience by node redundant water pressure, assuming higher redundant pressure indicates greater resilience. A representative indicator is Todini's (Todini, 2000) residual energy index, which focuses on the system's inherent ability to overcome adverse conditions without considering uncertainties. However, it fails to reflect network topology or post-damage recovery. To address this, scholars improved indicators by incorporating network balance and loop characteristics (Prasad et al., 2004; Farahmandfar et al., 2018; Jayaram et al., 2010): Huang et al. (2025) proposed node secondary neighborhood-based energy indicators (NRI_{2u}, NRI_{2uk}); Caetano et al. (2025) introduced the loop diameter uniformity coefficient (CRI) to the Todini index for more accurate reflection of redundant energy's contribution to resilience. Nevertheless, post-disaster recovery remains unaddressed. (3) The complex network method, based on graph theory, simplifies WDNs into nodes and edges, measuring topological robustness via average path length, connectivity, and independent loops (Yazdani et al., 2011; Assad et al., 2019; Selicato et al., 2024; Meng et al., 2018). It identifies structural vulnerabilities but is limited to static topology, ignoring functional attributes and dynamic post-disaster recovery. Yu et al. (2024) summarized graph theory applications in WDNs, suggesting combining graph theory and hydraulic indicators to improve assessment. (4) The recovery simulation method calculates WDN damage and recovery performance functions via full-process hydraulic analysis, defining resilience by integrating the system performance recovery curve within a control period based on the "resilience triangle" concept (Cimellaro et al., 2015; Liu

https://doi.org/10.5194/egusphere-2025-5830
Preprint. Discussion started: 14 January 2026

et al., 2020; Song et al., 2022; Sun et al., 2015; Bata et al., 2022). It well reflects dynamic post-disaster recovery but requires extensive, time-consuming hydraulic calculations and only provides overall results without local optimization guidance. In summary, selecting appropriate methods and indicators is a key challenge for quantitative WDN seismic resilience evaluation (Sakai, 2024). Table 1 lists representative quantitative indicators, advantages, and disadvantages of these four methods.

Table 1 A summary of indicators for assessing the seismic resilience of WDNs

Evaluation Indicator	Quantitative Indicators	Representative Scholars	Advantages and Disadvantages
Indicator-based method	$F_1(t)=1-\frac{\sum_i n_{ip,e}}{n_{Tot}}$; $R=\int_0^{T_{LC}}\frac{\overline{F_1}(t)}{T_{LC}}dt$	(Cimellaro et al., 2016)	Adv.: Simple and easy to implement. Disad.: Relies on subjective experience.
Energy-based method	$I_r=\frac{\sum_{i=1}^{n}q_i^*(h_i-h_i^*)}{\sum_{k=1}^{n_r}Q_kH_k+\sum_{j=1}^{n_p}\frac{P_j}{\gamma}-\sum_{i=1}^{n_n}q_i^*h_i^*}$	(Todini, 2000)	Adv.: Only requires focusing on the system's intrinsic ability to overcome adverse conditions, without considering various uncertainties. Disad.: Difficult to reflect the network's topological properties and does not account for post-damage recovery characteristics.
	$C_j=\frac{\sum_{i=1}^{n_{pi}}D_i}{np_j\cdot\max\{D_j\}}$	(Prasad et al., 2004)	
	$MI_r=\frac{\sum_{i=1}^{n}q_i^*(h_i-h_i^*)}{\sum_{i=1}^{n_n}q_i^*h_i^*}$	(Jayaram et al., 2010)	
	$C_u=\frac{n_p,withloop}{n_p}\cdot\frac{\sum_{i=1}^{n_l}C_l}{n_l}$	(Creaco et al., 2014)	
Complex network method	$q=\frac{2m}{n(n-1)}$	(Yazdani et al., 2011; Torres et al., 2017)	Adv.: Can reveal potential weak points in the network's structural level. Disad.: Remains at the static topological level, does not consider the system's functional attributes, and is difficult to capture the post-disaster dynamic recovery process.
	$k=\frac{2m}{n}$	(Yazdani et al., 2011; Fang et al., 2017; Hwang et al., 2017)	
	$l_T=\frac{1}{n(n-1)}\cdot\sum_{i,j}d(v_i,v_j)$	(Prose et al., 2016; Yazdani et al., 2012)	
	$C_i=\frac{2E_i}{k_i(k_i-1)}$	(Prose et al., 2016)	
	$BC(u)=\sum_{s\neq u\neq t}\frac{\sigma_{st}(\mu)}{\sigma_{st}}$	(Gathoklis et al., 2017)	
Recovery simulation method	$R_i=\int_0^{T_{LC}}\frac{F_i(t)}{T_{LC}}dt\ (i=1,2,3)$; $R=R_1\cdot R_2\cdot R_3$	(Cimellaro et al., 2016)	Adv.: Focuses on the system's dynamic recovery process after an earthquake. Disad.: Requires extensive hydraulic calculations, which are time-consuming, and only provides an overall assessment
	$NSD_i(t)=\begin{cases}1 & h_i(t)\geq h_{i0}(t)\\ \frac{h_i(t)}{h_{i0}(t)} & h_i(t)<h_{i0}(t)\end{cases}$; $SDI(t)=\sum_{i=1}^{n}w_i(t)NSD_i(t)$;	(Liu et al., 2020)	

https://doi.org/10.5194/egusphere-2025-5830
Preprint. Discussion started: 14 January 2026

$RI = \frac{1}{t_2 - t_1}\int_{t_1}^{t_2} SDI(t)dt$		without guidance for local optimization.
$R = \frac{\sum_{i=1}^{N_n}(\frac{1}{2}\cdot\sum_{j=1}^{N_i}(1-P_{fj})\cdot Q_i)}{4\cdot\sum_{i=1}^{N_n}Q_i}$	(Farahmandfer et al., 2016)	
$WSA_t = \sum_{n\in N}V_{nt} / \sum_{n\in N}V_{nt}$;	(Long et al., 2025)	
$PI_t = \sum_{n\in N}POP_n\delta_{nt};\ \delta_{nt} = \begin{cases}1 & \text{if } V_{nt}/V_{nt} < \tau \\ 0 & \text{otherwise}\end{cases}$		

In summary, while significant progress has been made in WDN resilience theory and methods, two limitations remain: (1) Temporally, stage divisions inconsistent with actual earthquake processes fail to accurately reflect the dynamic evolution of the entire seismic resilience process, especially lacking quantitative analysis of adaptation during the long-term post-disaster enhancement stage; (2) Functionally, mainstream indicator systems tend to be simplistic (Leštáková et al., 2023; Shuang et al., 2019), and no quantitative indicator system for multi-stage resilience assessment has been established, preventing comprehensive quantitative analysis of WDN seismic resilience and failing to meet the needs of disaster prevention, mitigation, and system optimization.

To address these limitations, this study establishes a four-stage framework that encompasses the entire seismic process of water distribution networks (WDNs), explicitly defining the onset, termination, and key characteristics of each stage. On this basis, a multi-dimensional indicator system is developed to quantify the seismic resilience of WDNs from multiple perspectives, including topological configuration, energy redundancy, pipeline resistance, hydraulic service performance, and recovery duration. This framework enables a systematic and refined assessment of resilience characteristics across all stages. Furthermore, this study reveals the variations in resilience across different stages and applies the proposed framework to support intervention decisions, thereby providing a scientific basis for optimizing network configuration and enhancing urban disaster prevention and mitigation capacity.

2 Four stages and resilience characteristics of WDNs in response to earthquakes

An examination of the entire damage and recovery process of water distribution networks (WDNs) during past earthquakes reveals that network disruption and restoration are not “one-time events” but evolve through multiple stages. For instance, after the 1995 Hanshin Earthquake, full water supply recovery in Kobe City required approximately 90 days (Kuraoka et al., 1996). Following the 2008 Wenchuan Earthquake, emergency water supply vehicles and temporary pipelines were deployed in the short term, while long-term recovery involved network renovation, seismic standard upgrades, and personnel training. These observations demonstrate that the manifestation of WDN seismic resilience is inherently dynamic, with

https://doi.org/10.5194/egusphere-2025-5830
Preprint. Discussion started: 14 January 2026

distinct characteristics, objectives, and dominant mechanisms at different stages of seismic disturbance. Based on an in-depth analysis of WDN damage and recovery processes in twelve earthquake-affected cities—including Mianzhu and Chengdu—this study categorizes the evolution of WDN functionality before and after an earthquake into four sequential stages (Liu & Zhang, 2013), and define the resilience characteristics corresponding to each stage.

2.1 Pre-disaster preparedness stage: Preparedness

The pre-disaster preparedness stage refers to the period prior to an earthquake, typically within one year, during which measures such as developing seismic codes, reinforcing vulnerable pipelines, replacing aging materials, stockpiling emergency supplies, and training repair personnel are implemented. During this stage, WDN resilience is primarily reflected in preparedness, defined by Keim (2008) as "activities and measures taken in advance to effectively respond to future disaster impacts." Its essence lies in structural rationality and resource availability. The system needs to identify critical vulnerable nodes and pipelines through vulnerability assessment, and evaluate topological redundancy and energy reserve capacity. Accordingly, this study defines preparedness as the system's capacity to maintain functionality despite failures of vulnerable components or insufficient energy, achieved through rational network topology and sufficient energy reserves.

At the node level, a node importance index is proposed, accounting for local connectivity and water demand proportion; nodes with high demand and low connectivity are identified as critical vulnerabilities. At the system level, the Gini coefficient quantifies disparities in node vulnerability, with smaller values indicating a more balanced and rational network structure. Resource redundancy is characterized by the network's remaining energy; higher energy availability reflects greater system resilience.

2.2 In-disaster resistance stage: Robustness

The in-disaster resistance stage occurs during the main earthquake and aftershocks, usually lasting from several seconds to hours, during which WDNs performance undergoes drastic changes under seismic action, typically showing varying degrees of decline. Pipelines, valves, instrumentation, and water treatment plant structures experience seismic-induced displacements and deformations. Excessive deformation often causes pipeline ruptures, joint leakage, and structural tilting or collapse. During this stage, WDN resilience is primarily reflected in robustness, which highlights the system's capacity to resist and absorb seismic impacts. Its main objective is to minimize structural damage while maintaining service levels. Robustness is defined as the WDN's ability to withstand disruptions and minimize service performance loss under seismic loading.

Robustness relies not only on the seismic strength of individual components but also on the system's capacity to sustain operations under partial damage. To address this, spatial variability of ground motion and intensity uncertainty are considered in WDN damage simulations. Evaluation indicators include average pipeline seismic damage rate and post-disaster water supply satisfaction; superior performance in these metrics reflects greater system robustness.

https://doi.org/10.5194/egusphere-2025-5830
Preprint. Discussion started: 14 January 2026

2.3 Post-disaster recovery stage: Recoverability

The post-disaster recovery stage starts from the end of the earthquake, this stage lasts approximately 3 days to 3 months (3d~12 weeks), with the goal of quickly restoring basic WDNs water supply capacity and ensuring drinking water safety and accessibility. Typical measures include deploying emergency water vehicles, installing temporary pipelines, and swiftly detecting and repairing leaks in critical pipelines. During the post-disaster short-term recovery stage, WDN resilience is primarily reflected in recoverability, highlighting the system's ability to rapidly restore service functions via component repair, resource allocation, and operational adjustments. Recoverability is defined as the system's capacity to quickly return to pre-disaster functional levels.

It focuses on meeting basic post-disaster urban water demand (to measure short-term recovery capacity), rather than in-depth functional recovery or structural optimization. Recoverability is defined as the system's capacity to quickly return to pre-disaster functional levels. Therefore, this study confines the short-term recovery stage to restoration of pre-disaster service levels. Evaluation indicators include WDNs recovery rate and service performance restoration, with faster recovery and higher restored performance indicating greater system recoverability.

2.4 Long-term enhancement stage: Adaptation

Long-term enhancement stage begins after short-term recovery, this stage lasts several months to years (typically 3 months to 3 years or longer). Objectives include full facility repair, replacement of damaged pipelines, enhancement of seismic standards, increased network redundancy, improved system monitoring, and personnel training. The long-term enhancement stage is characterized by adaptation. Adaptation emphasizes the system's ability to learn from disasters and, aligned with urban reconstruction and development planning, improve future seismic response through structural modifications and resource upgrades. It is defined here as the ability of WDNs to strengthen future earthquake response by modifying topology or augmenting energy reserves.

Adaptation primarily involves WDNs structural optimization and key component enhancement, focusing on future risk mitigation and integration with urban development. Ductility enhancement and network expansion strategies (Zhao et al., 2015) are employed to assess post-renovation changes in preparedness, robustness, and recoverability, thereby quantifying WDN adaptation under various interventions.

https://doi.org/10.5194/egusphere-2025-5830
Preprint. Discussion started: 14 January 2026

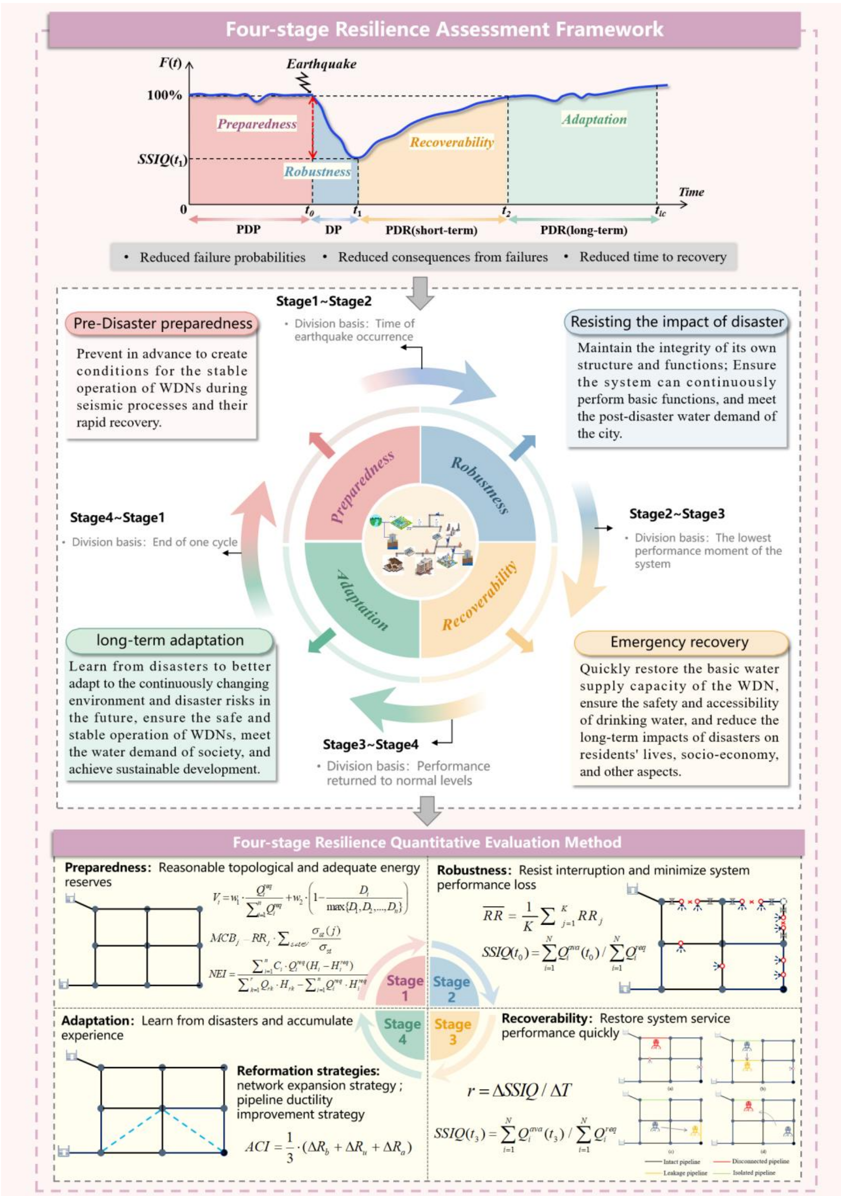

Fig.1 Four-Stage framework for seismic resilience assessment of Water Distribution Networks

3 Quantitative method for four-stage resilience of WDNs

Based on the Chapter 2, a four-stage seismic resilience assessment framework for WDNs is proposed (Fig. 1). Across the four stages of earthquake response, WDNs exhibit resilience characteristics of preparedness, robustness, recoverability, and adaptation. Resilience quantification at each stage is conducted using indicators derived from WDN attributes, including topology, energy redundancy, pipeline unit strength,

https://doi.org/10.5194/egusphere-2025-5830
Preprint. Discussion started: 14 January 2026

hydraulic performance, and recovery time. The main components of the methodology are summarized as follows. The process of four-stage quantitative assessment can be specifically illustrated in Fig. 4.

3.1 Construction of earthquake damage scenarios

First, the post-disaster damage state of WDNs is determined using the WDN seismic fragility model and ground motion attenuation model. Monte Carlo Simulation (MCS) is employed to incorporate uncertainties in seismic damage. Finally, post-disaster WDN performance is assessed via hydraulic simulation results. The workflow is illustrated in Fig. 2.

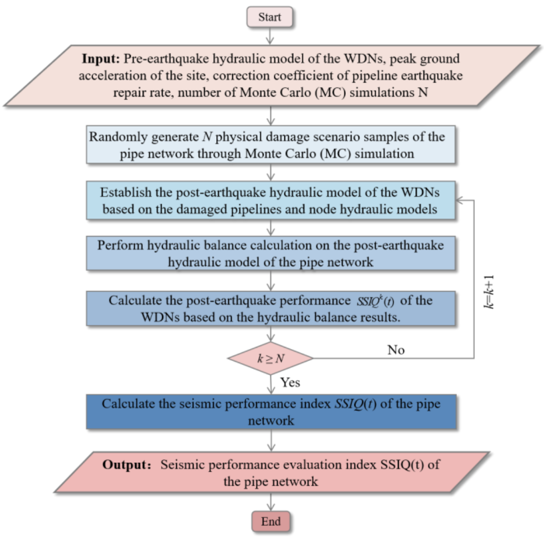

Fig. 2 Construction of earthquake damage scenarios

3.1.1 Seismic hazard analysis

Seismic hazard analysis involves scientifically assessing the potential seismic impact an engineering site may experience over future time horizons. Commonly applied approaches include deterministic and probabilistic methods. Probabilistic Seismic Hazard Analysis (PSHA) (Jayaram et al., 2010; McGuire, 2008) assumes that temporal, spatial, and intensity characteristics of future seismic events, as well as regional intensity levels, are inherently stochastic. Results are typically expressed as exceedance probabilities of site-specific intensity measures or ground motion parameters. This study employs the ground motion attenuation model by Toro et al. (1997) to compute the Peak Ground Acceleration (*PGA*) at each pipeline, as given by the following formula:

$$
\begin{aligned}
\ln PGA &= 2.20 + 0.81\cdot\left(M_w\text{-}6\right) - 1.27\ln\sqrt{R_{jb}^2 + 9.3^2} \\
&+0.11\cdot\max\left[\ln\left(\frac{\sqrt{R_{jb}^2+9.3^2}}{100},0\right)\right] - 0.0021\cdot\sqrt{R_{jb}^2+9.3^2}
\end{aligned}
\tag{1}
$$

In the formula, *PGA* represents Peak Ground Acceleration (*g*); M_w is the moment magnitude; and R_{jb} denotes the shortest horizontal distance from the earthquake rupture.

https://doi.org/10.5194/egusphere-2025-5830
Preprint. Discussion started: 14 January 2026

3.1.2 Seismic fragility model of pipelines

A water distribution networks (WDNs) primarily comprises four components: water source, transmission, distribution, and consumption. It includes water intake pumping stations, water transmission pipelines, water treatment plants, water distribution pipelines, various valves and instruments, and other types of structures. Among these components, the water distribution pipeline network accounts for the largest proportion of the total assets of the entire WDN, usually approximately 60% to 80%. They are also the most vulnerable components during seismic events. Accordingly, this study focuses only on pipeline damage, neglecting impacts on secondary components such as pumping stations and valves.

The fragility model of water distribution pipelines is usually obtained by fitting historical seismic damage data. Damage is commonly quantified by the pipeline repair rate, defined as the number of damages per kilometer under a given seismic intensity. This study adopts the calculation formula proposed by Isoyama et al. (2000):

$$RR_0 = 2.88 \times 10^{-6} \times (980 \times PGA - 100)^{1.97} \tag{2}$$

$$RR = C_\mathrm{p} \times C_\mathrm{m} \times C_\mathrm{t} \times C_\mathrm{l} \times RR_0 \tag{3}$$

In the formula, RR represents the pipeline repair rate (locations per kilometer); C_p, C_m, C_t, and C_l represent the correction coefficients related to pipeline diameter, pipeline material, terrain, and site liquefaction degree, respectively, and their values please refer to literature (Isoyama et al., 2000).

Assuming that the number of damages occurring in each pipeline after an earthquake follows a Poisson distribution along the pipeline length L, the probability of n damages occurring in a pipeline is given by:

$$P(N_\mathrm{d} = n) = \frac{(RR \times L)^n}{n!} \times e^{-RR \times L} \tag{4}$$

In the formula, N_d represents the number of damages occurring in the pipeline; L is the length of the pipeline (km). Based on this formula, the probability of post-disaster pipeline damage can be derived as follows:

$$P_\mathrm{d} = 1 - P(N_\mathrm{d} = 0) = 1 - e^{-RR \times L} \tag{5}$$

3.1.3 Leakage model of water distribution networks

This study assumes that pipeline damage types include two categories: leakage and breakage, accounting for 80% and 20% of total damage, respectively. The leakage model for WDNs is illustrated in Figure 3. For pipelines with leakage (Figure 3(a)), a virtual pipeline with a check valve is introduced at the damage site, connecting a virtual node to a virtual reservoir (Figure 3(b)). For pipelines with breakage (Figure 3(c)), two virtual reservoirs are installed at the break point, linked to Nodes A and B via pipelines with check valves. Each connecting pipeline has a length of $L/2$, with diameter and material identical to the original pipeline AB (Figure 3(d)). The elevation of the virtual reservoirs is the same as that of the pipeline break location. Additional parameters are detailed in Reference (Han et al., 2020).

https://doi.org/10.5194/egusphere-2025-5830
Preprint. Discussion started: 14 January 2026

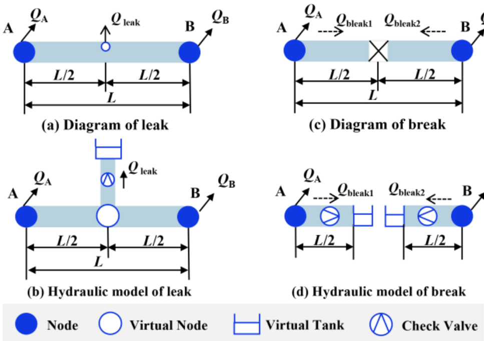

Fig. 3 Diagram and hydraulic model of pipeline damage

3.2 Preparedness quantification

First, key nodes and pipelines are identified using the node importance index (V_i) and betweenness centrality index (MCB_j). The Gini coefficient-based node homogeneity index (G_w) is employed to assess topological rationality and the disparity in node vulnerability. Second, available energy reserves are calculated to evaluate system redundancy. Finally, G_w and the energy index (NEI) serve as quantitative indicators of WDN preparedness.

Specifically, node importance is quantified from functional and structural perspectives, accounting for the node's water demand proportion and local connectivity. The node importance index (V_i) is calculated as follows:

$$V_i = w_1 \cdot \frac{Q_i^{req}}{\sum_{i=1}^{n} Q_i^{req}} + w_2 \cdot \left(1 - \frac{D_i}{\max\{D_1, D_2, ..., D_n\}}\right) \tag{6}$$

In the formula, V_i represents the importance index of Node i; Q_i^{req} represents the basic water demand of node i; n is the number of user nodes; D_i is the degree of node i, i.e., the number of pipelines connected to this node; $w_1$and w_2 are weight coefficients with $w_1+w_2=1$, which can be determined according to actual conditions and managers' requirements.

For the identification of key vulnerable pipelines, the assessment is conducted from two aspects: topology and pipeline resistance. The pipeline betweenness centrality index MCB_j, incorporating seismic hazard, is employed. Pipelines exhibiting high betweenness and high seismic damage probability are regarded as key vulnerable pipelines. The calculation formula is as follows:

$$MCB_j = RR_j \cdot \sum_{s \neq t \in V} \frac{\sigma_{st}(j)}{\sigma_{st}} \tag{7}$$

In the formula, MCB_j represents the importance index of Pipeline j; RR_j represents the seismic damage rate of Pipeline j under the current design-basis earthquake intensity; V is the set of all nodes in the topological structure of the water distribution network; σ_{st} is the number of shortest paths from Node s to Node t; and $\sigma_{st}(j)$ is the number of shortest paths from Node s to Node t that pass-through Pipeline j.

At the network level, the Gini coefficient (G_w), derived from node importance, is employed to evaluate

https://doi.org/10.5194/egusphere-2025-5830
Preprint. Discussion started: 14 January 2026

network structural rationality. G_w ranges from 0 to 1; the closer G_w is to 0, values closer to 0 indicate more uniform node vulnerability and a more rational network structure. The G_w calculation is given by the following formula:

$$G_w = \frac{1}{2N^2\overline{V}}\sum_{i=1}^{N}\sum_{j=1}^{N}\left|V_i - V_j\right| \tag{8}$$

In the formula, N represents the total number of user nodes; V_i is the node importance of node i; and $\overline{V}$ is the average value of node importance across all user nodes.

System energy reserve is quantified using the Todini index, which accounts for pipeline diameter uniformity (Huang et al., 2025). Higher index values correspond to greater WDN energy reserves. The index is calculated as follows:

$$NEI = \frac{\sum_{i=1}^{n} C_i \cdot Q_i^{req}(H_i - H_i^{req})}{\sum_{k=1}^{r} Q_{rk} \cdot H_{rk} - \sum_{i=1}^{n} Q_i^{req} \cdot H_i^{req}} \tag{9}$$

$$C_i = \frac{\sum_{j \in P_i} d_j}{n_{pi} \cdot \max\{d_1, d_2, ..., d_j\}} \tag{10}$$

In the formula, NEI represents the energy index considering pipeline diameter uniformity; H_i represents the actual water pressure at node i; H_i^{req} represents the required water pressure at node i; r is the number of water sources; Q_{rk} denotes the output water quantity of water source k; H_{rk} is the total head of water source k; C_i represents the uniformity coefficient; P_i represents the set of pipelines connected to node i; d_j is the diameter of pipeline j(mm); and n_{pi} denotes the number of pipelines connected to Node i.

3.3 Robustness quantification

First, probabilistic seismic hazard analysis (PSHA) is applied to estimate the peak ground acceleration (PGA) at each pipeline location in the WDNs. Monte Carlo simulation (MCS) is then employed to account for seismic damage uncertainty, establishing a physical damage model for the WDN. The robustness of the WDNs is assessed from two perspectives: individual pipeline resistance and overall hydraulic service performance. Finally, two quantitative indicators are adopted: the average post-disaster pipeline seismic damage rate $\overline{RR}$ and the system service water adequacy quotient at the initial post-disaster state, $SSIQ(t_1)$.

Specifically, for individual pipeline resistance, the seismic damage rate of each pipeline is first obtained using Eq. (3). Subsequently, the average seismic damage rate of all pipelines in the WDNs is then calculated as follows:

$$\overline{RR} = \frac{\sum_{j=1}^{K} RR_j}{K} \tag{11}$$

In this formula, $\overline{RR}$ represents the average seismic damage rate of the pipelines; K represents the total number of pipelines in the network; RR_j is the seismic damage rate of of pipeline j, which is derived from Eq. (4).

https://doi.org/10.5194/egusphere-2025-5830
Preprint. Discussion started: 14 January 2026

To evaluate the post-disaster service performance of the WDNs, this study adopts the demand-based performance indicator proposed by Liu et al. (2020). The water supply satisfaction indicator *SSIQ* is defined as the ratio between the total actual water delivered to all user nodes after a disturbance and the total baseline demand under normal operating conditions. The indicator is defined as follows:

$$SSIQ(t) = \frac{\sum_{i=1}^{N} Q_i^{ava}(t)}{\sum_{i=1}^{N} Q_i^{req}} \tag{12}$$

In this equation, *SSIQ* represents the performance indicator of the WDNs at time t; i represents the water-demanding node i; N is the total number of water-demanding nodes in the WDNs; Q_i^{ava} stands for the actual water distribution volume at water-demanding node i at time t (L/s); Q_i^{req} represents the basic water demand volume of water-demanding node i (L/s). This study assumes that the baseline water demand at each consumption node remains constant and is unaffected by disturbances such as earthquakes. Under normal pre-disaster conditions, the actual supply at each node equals its baseline demand, resulting in an initial water supply satisfaction ($SSIQ_0$) of 1. Here, t_1 refers to the time when the WDNs performance drops to its lowest point after the earthquake.

3.4 Recoverability quantification

In the short-term recovery stage, this study models only pipeline restoration, assuming that restoration activities fall into three categories: isolation, replacement, and repair. First, the restoration sequence of damaged pipelines is determined, followed by hydraulic simulations of the recovery process for the damaged WDNs. Second, based on the simulated recovery process, the WDN's recovery extent and rate are evaluated. Finally, two quantitative indicators are adopted to assess recoverability: (1) the water supply satisfaction index, $SSIQ(t_3)$, representing WDN performance after three days of restoration, and (2) the network recovery rate, r.

Specifically, for the restoration of broken pipelines, the damaged section is first isolated and then replaced. In contrast, for leaking pipelines, only repair operations are needed to restore them to normal service conditions. The restoration time of a pipeline is determined by both the type of damage and the pipeline diameter, and it is calculated as follows:

$$T = \begin{cases} 0.25 \cdot n_{value}, & \text{isolation} \\ 0.156 \cdot D^{0.719}, & \text{replacement} \\ 0.223 \cdot D^{0.577}, & \text{reparation} \end{cases} \tag{13}$$

In this equation, n_{value} denotes the number of isolation valves required for isolating broken pipelines.

Second, the restoration sequence of damaged pipelines has a direct impact on the recovery rate and overall resilience of the system. In real post-disaster recovery processes of water distribution networks (WDNs), various factors—such as the availability of maintenance resources and administrative directives—introduce considerable uncertainty. Hence, this study adopts a simplified approach to simulate the recovery process of WDNs, focusing on the recovery strategy determined by the static importance of each pipeline.

https://doi.org/10.5194/egusphere-2025-5830
Preprint. Discussion started: 14 January 2026

The static importance of a pipeline ($I_{s,j}$) is calculated as follows:

$$I_{s,j} = \frac{1}{T_j}(SSIQ_j - SSIQ_0) \tag{14}$$

In the formula, $I_{s,j}$ denotes the static importance index of pipeline *j*; T_j represents the repair time of pipeline *j*; and $SSIQ_j$ is the water distribution network service performance index after the repair of pipeline *j*. It can be inferred from the formula that ($SSIQ_j$-$SSIQ_0$) stands for the improvement of the network service performance brought by the repair of pipeline *j*, and this improvement is a key parameter reflecting the importance of pipeline *j*. For two pipelines with the same improvement in network service performance, the one with shorter repair time not only facilitates the promotion of subsequent pipeline repair work, but also accelerates the improvement of the overall service performance of the system.

Finally, to quantify the recovery efficiency of the WDNs, the recovery rate is defined in this study as the ratio of the service performance improvement value of the damaged network to the total recovery time during the recovery process. The calculation formula for the WDN recovery rate *r* is as follows:

$$r = \frac{\Delta SSIQ}{\Delta T} \tag{15}$$

In the formula, $\Delta SSIQ$ denotes the service performance improvement value of the damaged water distribution network during the post-disaster recovery stage; ΔT represents the total recovery time.

3.5 Adaptation evaluation

In this stage, based on the multi-dimensional evaluation indicators established in the previous three stages, this study enhances the resilience of the WDNs from two perspectives: the network's topological structure and the seismic resistance of its pipeline components. Specifically, two enhancement strategies are implemented: a network expansion strategy and a pipeline ductility improvement strategy (Zhao et al., 2015). Subsequently, seismic damage simulations are performed again on the WDN after the implementation of these renovation measures to evaluate the network's resilience preparedness, robustness, and recoverability. The total improvement in resilience indices across all stages serves as the criterion for assessing the effectiveness of each renovation strategy. Finally, the average comprehensive improvement rate (*ACI*) of the indicators is introduced as a measure of the overall adaptation of the WDNs.

Specifically, based on the network expansion and pipeline ductility improvement strategies, this study implements three seismic retrofitting measures for the water distribution network: critical pipeline ductility enhancement (S1), network expansion (S2), and combined retrofitting (S3). For each retrofitting measure, the average comprehensive improvement rate (*ACI*) of each network indicator is calculated as follows:

$$\Delta R_k = \sum_{m=1}^{M} \theta_{k,m} \cdot C_m \cdot (1 - R_k^0) \quad k \in \{b, u, a\} \tag{16}$$

$$ACI = \frac{1}{3} \cdot (\Delta R_b + \Delta R_u + \Delta R_a) \tag{17}$$

https://doi.org/10.5194/egusphere-2025-5830
Preprint. Discussion started: 14 January 2026

In the formula, k represents the stage index(b is preparedness, u is robustness, a is recoverability); C_m represents the implementation intensity of retrofit measure m (S1,S2,S3) ; $\theta_{k,m}$ is the corresponding enhancement coefficient for stage k; R_k^0 is the baseline resilience level, and (1- R_k^0) accounts for the remaining improvement potential; ACI represent the adaptation index, defined as the weighted sum of the improvement rates across all stages.

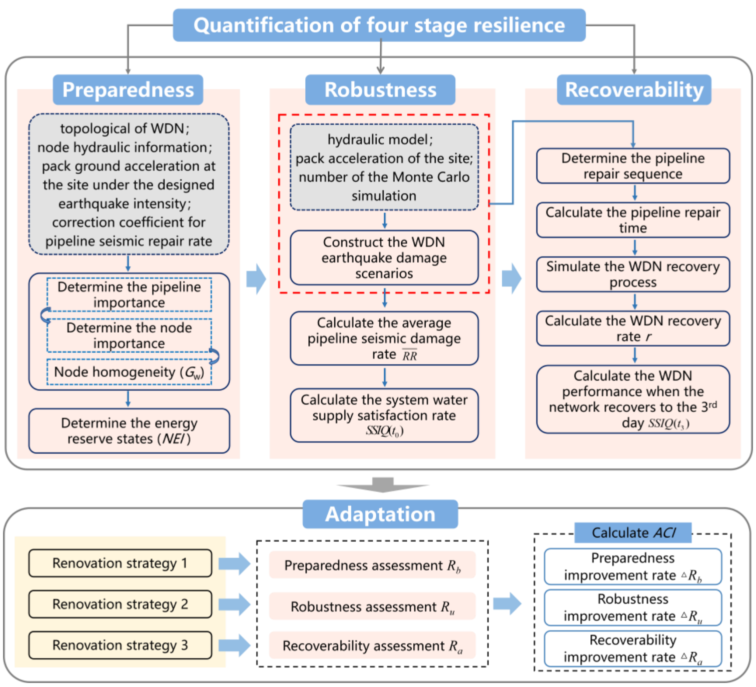

Fig. 4 Four-stage quantitative assessment flowchart

4 Case study

4.1 Overview of case networks

This study evaluates the proposed method through two case studies: a small-scale water distribution network (Jilin WDN) and a larger, more complex network (Mianzhu WDN) (Fig. 5). (1) Jilin WDN: It comprises 27 nodes, 34 distribution pipelines (average diameter: 266 mm), and a water treatment plant as the source. (2) Mianzhu WDN: It serves an area of approximately 25 km² and a population of about 80,000. After simplification, the WDN includes 107 pipelines, 78 nodes, and two water treatment plants. Water plant R1 supplies an average of 16,000 tons of water daily, while water plant R2 supplies about 24,000 tons daily. Both WDNs use only two types materials: cast iron and plastic pipelines.

https://doi.org/10.5194/egusphere-2025-5830
Preprint. Discussion started: 14 January 2026

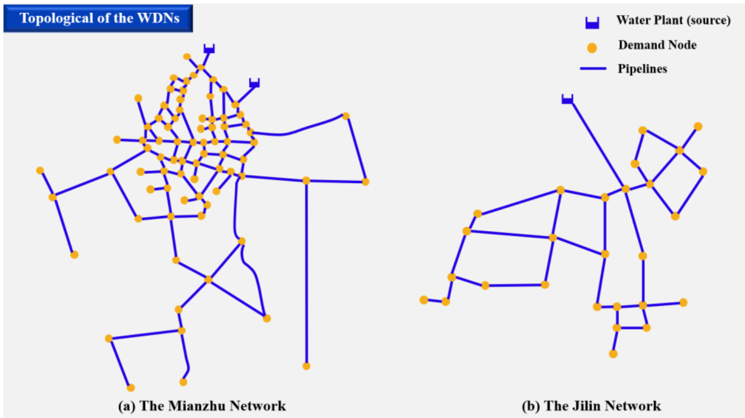

Fig. 5 Topology schematic of the case networks

4.2 Four-Stage seismic resilience assessment

4.2.1 Preparedness assessment

During the pre-disaster preparation stage, the importance index (V_i) of each node in both case WDNs was assessed using Eq. (6) under the assumption that w_1=w_2. The Gini coefficient (G_w) was employed to evaluate the homogeneity between the structural and functional importance of nodes within the entire network. The energy redundancy of the two WDNs was then verified, with results presented in Fig. 6. The key findings are as follows: (1) The Network Energy Index (*NEI*) for both Jilin and Mianzhu WDNs are similar, indicating comparable energy reserves. (2) At the system level, the Gini coefficient of Mianzhu WDN is significantly higher than that of Jilin WDN, indicating notable differences in node importance distribution. This suggests that Mianzhu WDN has many vulnerable nodes with high water demand but poor local connectivity, increasing its susceptibility to service disruptions during disasters. (3) The difference between the two indicator evaluation results indicates that solely considering system energy redundancy cannot significantly improve preparedness. Although the Mianzhu WDN shows a slight advantage in energy reserves, its network imbalance may still lead to local instability or water supply interruptions after an earthquake.

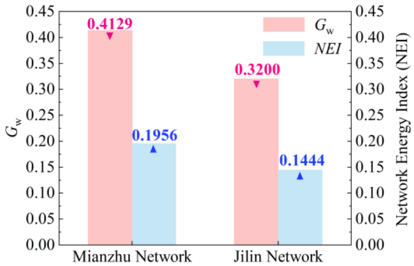

Fig. 6 Nodes homogeneity and energy redundancy of WDNs

To further clarify the spatial distribution of critical components within the WDN and guide subsequent optimization decisions, Fig. 7 shows the spatial distribution of component importance in the two WDNs,

https://doi.org/10.5194/egusphere-2025-5830
Preprint. Discussion started: 14 January 2026

highlighting the key nodes and pipelines ranked within the top 10% of importance. In both WDNs, the key nodes are primarily located along the network periphery. Compared with other nodes, these peripheral ones have fewer pipeline connections and are more susceptible to service interruptions caused by seismic-induced pipeline damage. In the Mianzhu WDN, for instance, the water demands of Nodes 76 and 78 are 9.6 times higher than the network average (5.15 L/s), making them critical targets for optimization and maintenance. Identifying and reinforcing these vulnerable key components are essential for enhancing the overall seismic resilience of WDNs.

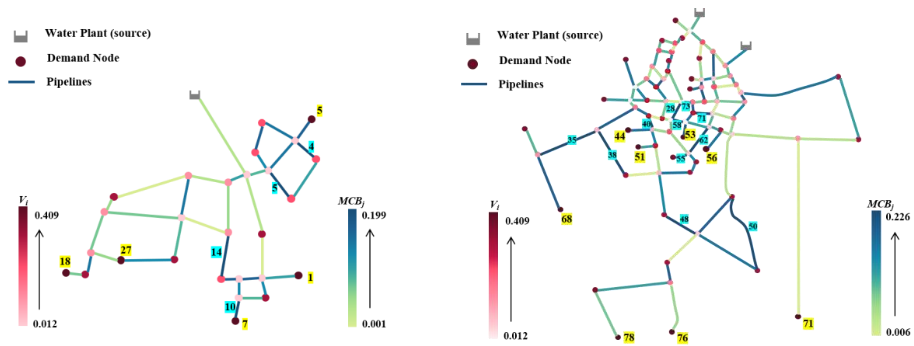

(a) The Jilin WDN (a) The Mianzhu WDN

Fig. 7 Spatial distribution of WDNs component importance (The darker the color, the higher the importance of the component. For the identification of key pipelines, it is assumed that the current seismic fortification intensity is X)

4.2.2 Robustness assessment

In this study, seismic hazard analysis was conducted, incorporating the effect of spatial incoherence of the ground motion field, to determine the distribution of peak ground acceleration (PGA) along each pipeline. Figure 8(a) depicts the spatial distribution of the ground motion field at the Mianzhu WDN site, whereas Figures 8(b) and 8(c) show the corresponding PGA distributions for the Jilin and Mianzhu WDNs under a scenario earthquake of M_w =7.0.

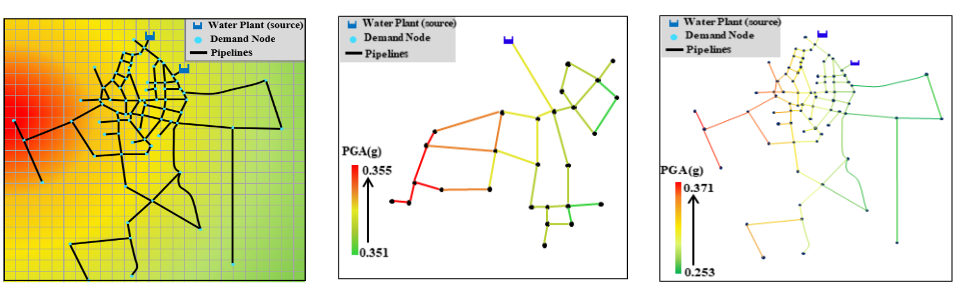

(a) spatially non-uniform ground motion field (b) PGA Spatial Distribution of the Jilin WDN (c) PGA Spatial Distribution of the Mianzhu WDN

Fig. 8 Seismic Hazard Analysis of WDNs (The seismic source is located 20 km west of the network,

https://doi.org/10.5194/egusphere-2025-5830
Preprint. Discussion started: 14 January 2026

with a depth of 10 km)

Based on Eq. (10), the variation curves of the average seismic damage rate for the two case WDNs were obtained, as illustrated in Figure 9. It can be observed that the Jilin WDN exhibits a higher average seismic damage rate than the Mianzhu WDN, and the difference gradually increases with earthquake intensity. Under an Mw 8.0 earthquake, in particular, the average seismic damage rate of the Jilin WDN reaches 0.740, which is markedly higher than 0.576 for the Mianzhu WDN. This can be mainly attributed to the relatively smaller pipeline diameters in the Jilin WDN, which result in a higher overall seismic damage rate.

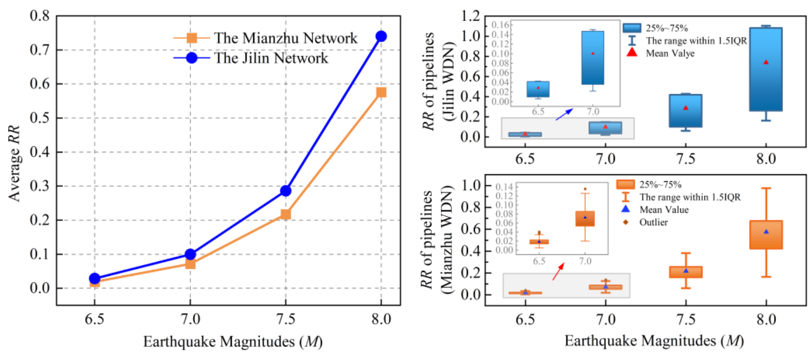

Fig.9 Average seismic damage rate of pipelines under different magnitudes (The boxplot on the right shows the distribution of the seismic damage rate *RR* for each pipeline under different magnitudes)

Furthermore, the Monte Carlo simulation method was employed to perform 200 earthquake damage scenarios for the two case WDNs. The water supply satisfaction index of the overall WDN in the initial post-disaster state ($SSIQ(t_0)$), together with that of each demand node (SIQ_i), was statistically analyzed. Fig. 10 presents the post-disaster water supply satisfaction for the two WDNs. In terms of water supply performance, the satisfaction index of the Jilin WDN remains higher than that of the Mianzhu WDN across all earthquake magnitudes. According to the Guidelines for Seismic Resilience Assessment of Urban Engineering Systems (RISN-TG041-2022, 2022), a performance threshold of 0.45 was adopted for the WDNs in this study. It can be observed that when the earthquake magnitude exceeds 7.5, both the Jilin and Mianzhu WDNs lose their fundamental service functionality. At the nodal level, under small to moderate earthquakes, the water supply satisfaction indices in both WDNs are relatively concentrated. Under major earthquakes, however, the distribution becomes more dispersed, indicating larger performance disparities among nodes. Under an M_w 8.0 earthquake, the mean nodal satisfaction falls below the median, indicating a pronounced degradation in overall service performance and a substantial proportion of low-performing nodes within the WDN.

The robustness assessment reveals a nonlinear relationship between pipeline resistance and system hydraulic performance. Although the Mianzhu WDN exhibits a lower average pipeline damage rate than the Jilin WDN, its post-earthquake hydraulic service performance ($SSIQ(t_0)$) is comparatively poorer. This indicates that system robustness depends not only on the seismic strength of individual pipelines but also on the system's overall ability to maintain flow distribution and pressure balance under damaged conditions.

https://doi.org/10.5194/egusphere-2025-5830
Preprint. Discussion started: 14 January 2026

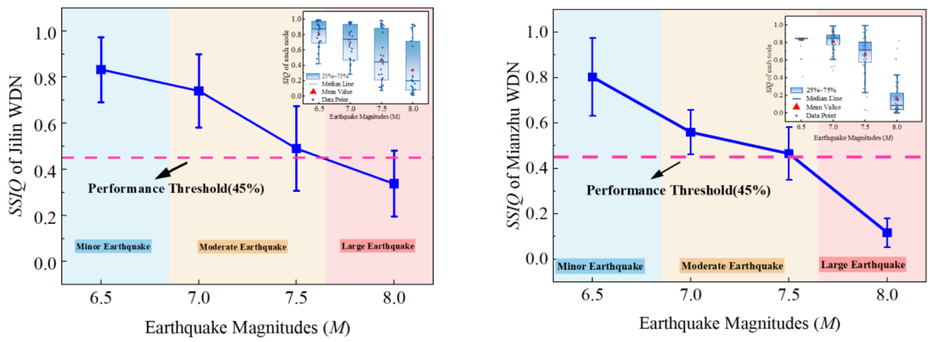

(a) The Jilin WDN (a) The Mianzhu WDN

Fig. 10 Water supply satisfaction rate under different magnitudes

4.2.3 Recoverability assessment

To evaluate the recoverability of the WDNs, a function-based static importance restoration strategy was adopted to simulate the post-disaster recovery process of the damaged networks. The recovery rate (*r*), recovery time (*RT*), and water supply satisfaction index on the third day of recovery ($SSIQ(t_3)$) were statistically analyzed for both WDNs. The results are summarized as follows: (1) In terms of recovery rate (Figure 11), the Jilin WDN exhibits a markedly higher recovery rate than the Mianzhu WDN, and this rate decreases with increasing earthquake magnitude. Under an M_w 6.5 earthquake, the recovery rates of the two WDNs reach 1.5352 and 1.0067, respectively, both notably higher than those under the other three magnitudes. (2) Figure 12 illustrates the mean performance recovery curves and their one-standard-deviation confidence intervals for the Mianzhu and Jilin WDNs under seismic events of different magnitudes. Under an M_w 7.0 earthquake, both networks show a rapid rise in *SSIQ* within 72 hours, reaching mean values above 0.90, indicating that most service functionality can be restored within three days. Under an M_w 7.5 earthquake, the mean *SSIQ* at 72 h decreases to about 0.6442 in Mianzhu and 0.9595 in Jilin, revealing a significant decline in short-term recovery efficiency due to more severe pipeline damage and prolonged restoration time. (3) The Mianzhu WDN presents wider uncertainty bands, particularly under the M_w 7.5 earthquake, suggesting greater variability and vulnerability in post-seismic recovery, which attributed to its complex topology and uneven redundancy. In contrast, the Jilin WDN exhibits narrower uncertainty ranges and higher $SSIQ(t_3)$, indicating more robust and predictable recovery performance.

The recovery-stage results indicate that the pre-disaster topological and energy conditions exert a significant feed-forward effect on post-disaster recovery capacity. Owing to its higher topological rationality and energy redundancy during the preparedness stage, the Jilin WDN achieves a markedly faster recovery rate (*r*) and higher water supply satisfaction ($SSIQ(t_3)$) than the Mianzhu WDN. This suggests that recoverability is not an independent stage-specific attribute but is jointly influenced by the system's pre-disaster preparedness and overall hydraulic performance.

https://doi.org/10.5194/egusphere-2025-5830
Preprint. Discussion started: 14 January 2026

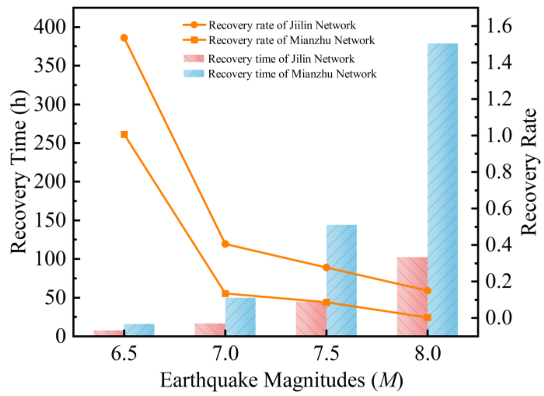

Fig. 11 The WDNs' recovery time and recovery rate under different magnitudes

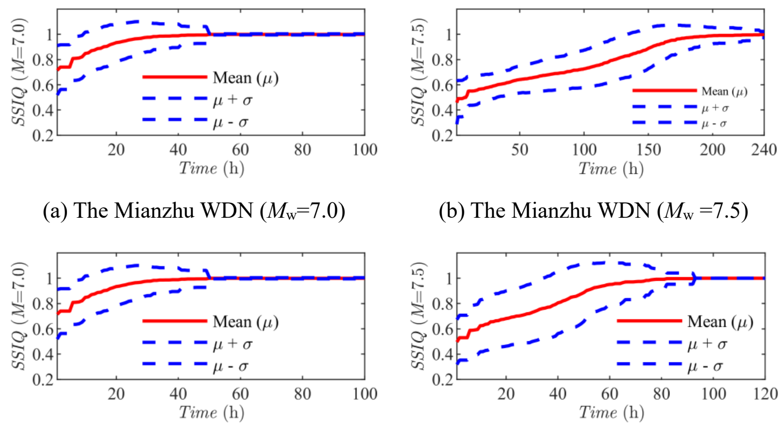

(a) The Mianzhu WDN (M_w=7.0) (b) The Mianzhu WDN (M_w =7.5)

(c) The Jilin WDN (M_w =7.0) (d) The Jilin WDN (M_w =7.5)

Fig. 12 Mean performance recovery curves and one standard deviation error bars of WDNs under different magnitudes

4.2.4 Adaptation assessment

In this study, two resilience enhancement strategies were implemented for the Jilin and Mianzhu WDNs: a network expansion strategy and a pipeline ductility enhancement strategy. Specifically, three renovation measures were applied to the case networks, as summarized in Table 2. Seismic damage simulations were then re-conducted on the renovated WDNs, and the improvement of each resilience index under different earthquake intensities was calculated to evaluate the adaptation of the enhancement strategies. Based on the key components identified in the preparedness stage and the results of the robustness analysis, the damage frequency of each pipeline in 200 Monte Carlo (MC) simulations was statistically analyzed, as illustrated in Fig. 13. Subsequently, the ductility enhancement strategy was applied to key pipelines and those exhibiting high failure probabilities (i.e., more than 50 failures in 200 simulations), while the network expansion

https://doi.org/10.5194/egusphere-2025-5830
Preprint. Discussion started: 14 January 2026

strategy was implemented for key nodes. The specific nodes and pipelines involved in the renovation are shown in Fig. 14.

Table 2 Seismic retrofit strategies for WDNs

No.	Retrofit Measures	Remarks
S1	Pipeline Ductility Enhancement Strategy	The original pipeline diameters were increased by 50 mm, and the cast iron pipelines (CIP) were replaced with ductile iron pipelines (DIP)
S2	Network Expansion Strategy	Additional pipeline connections were established at key nodes, and all newly added pipelines were ductile iron pipelines (DIP)
S3	Combined Retrofit Strategy	The pipelines of key pipelines were replaced and enlarged by 50 mm in diameter, while additional connections were introduced at key nodes

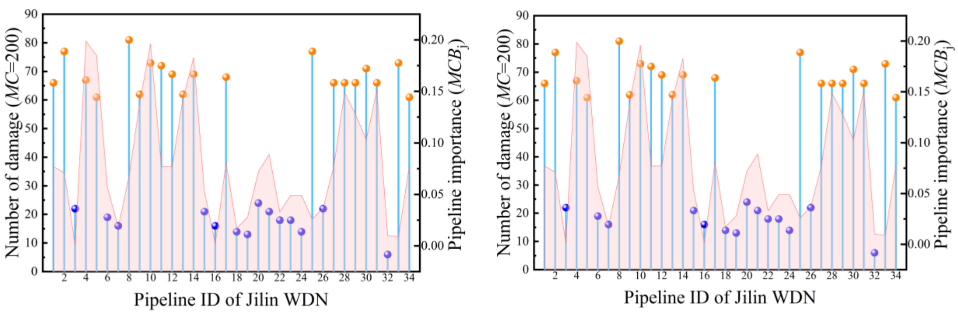

Fig. 13 Statistics on pipeline failure frequency

(Orange indicates the pipelines that are involved in the renovation)

The resilience of the WDNs at each stage under different renovation measures is shown in Fig. 15. The main findings are summarized as follows: (1) Under the ductility enhancement strategy, the adaptation index (ACI) of the Jilin WDN is 0.2013, whereas that of the Mianzhu WDN is only 0.0042, indicating that this strategy exerts a significant positive effect on the Jilin WDN. (2) Under the network expansion strategy, the adaptation index of the Jilin WDN is 0.0622, while that of the Mianzhu WDN reaches 0.0976. Either the ductility enhancement or network expansion strategy alone produces limited improvements in both WDNs; however, the Mianzhu WDN exhibits a more pronounced enhancement under the network expansion strategy. (3) When the two strategies are implemented simultaneously, the adaptation index of the Jilin WDN reaches 0.2785, while that of the Mianzhu WDN reaches 0.1396. It is evident that the combined retrofit strategy (S3) yields the greatest improvement in seismic resilience for the Jilin WDN, whereas its effect on the Mianzhu WDN remains relatively limited. (4) For the Mianzhu WDN, all three retrofit strategies exhibit limited effects on improving overall resilience. Nevertheless, implementing two strategies simultaneously provides better resilience enhancement than adopting a single strategy. This finding suggests that more tailored retrofit strategies should be developed to optimize seismic resilience based on the specific characteristics of different

https://doi.org/10.5194/egusphere-2025-5830
Preprint. Discussion started: 14 January 2026

WDNs.

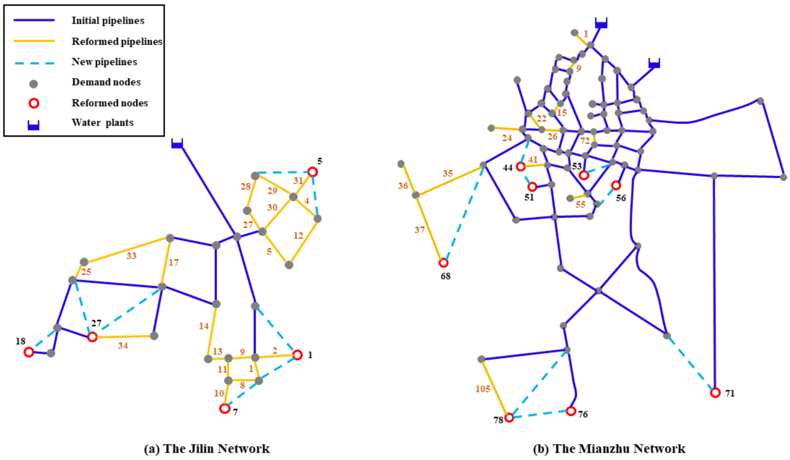

Fig. 14 Schematic Diagram of Retrofit Nodes and Pipelines

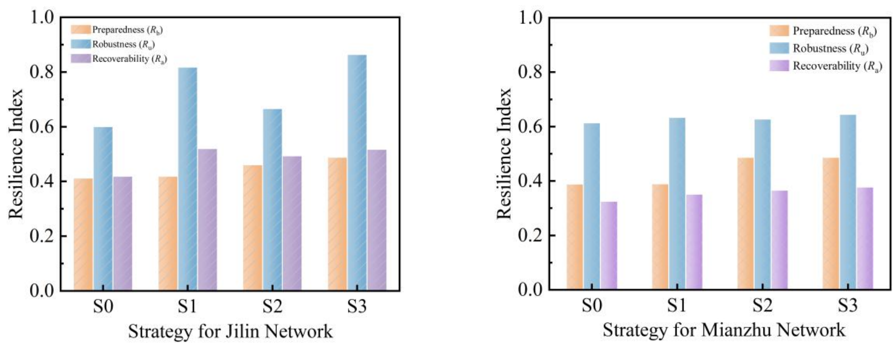

(a) The Jilin WDN (b) The Mianzhu WDN

Fig. 15 Resilience indices of WDN at various stages under different retrofit measures (S0 represents the resilience level of the initial WDNs)

5 Discussion

The proposed four-stage seismic resilience assessment framework for WDNs comprehensively captures the dynamic evolution of seismic resilience. Within the proposed framework, the quantitative assessment of preparedness, robustness, recoverability, and adaptation has been systematically achieved. The case studies revealed distinct differences in the four resilience dimensions among different WDNs, as well as the heterogeneous impacts of various retrofit strategies on enhancing seismic resilience. This framework offers a novel perspective and a practical methodology for the seismic design and optimization of WDNs.

5.1 Rationality verification of the four-stage assessment framework

To further validate the rationality of the proposed assessment framework, the stage-wise resilience levels of the two case WDNs were computed using a weighted summation of the stage-specific evaluation indices,

https://doi.org/10.5194/egusphere-2025-5830
Preprint. Discussion started: 14 January 2026

assuming equal weights for all indicators. These calculations were based on the results presented in Section 4. In addition, the evaluation results were compared with those derived from the conventional single-index method based on the system functionality recovery curve. The formula for evaluating the seismic resilience of WDNs using the conventional method is expressed as follows:

$$RI = \frac{1}{t_c - t_1}\int_{t_0}^{t_c} SSIQ(t)dt \tag{18}$$

In the formula, $SSIQ(t)$ represents the system performance function, with its specific calculation referring to Eq. (12); t_c represents the time at which the system performance recovers to the normal level; and t_1 is the time at which the restoration activities start.

When M_w =7.5, the resilience levels of each stage are presented in Table 3. It can be observed that, under the four-stage assessment framework, the robustness of the Mianzhu WDN is slightly superior to that of the Jilin WDN. This result is consistent with that obtained using the traditional Resilience Index (*RI*) method, with calculation errors of 0.084 and 0.082, respectively. Although the two WDNs exhibit comparable overall seismic resilience levels based on the traditional RI metric, their stage-specific performances differ markedly under the proposed four-stage framework. The Jilin WDN demonstrates outstanding recoverability, and when both the ductility enhancement and network expansion strategies are implemented simultaneously, its adaptation index reaches a maximum value of 0.2785. In contrast, the Mianzhu WDN shows a marginal advantage in robustness but relatively weaker preparedness and adaptation, with corresponding gaps of 0.0229 and 0.1389 compared to the Jilin WDN. Therefore, the proposed assessment framework can more comprehensively reveal the resilience disparities among different WDNs across the four seismic stages from a multi-attribute perspective. Compared with previous approaches that rely solely on a single hydraulic service performance indicator, this framework can explicitly characterize the resilience level of each seismic stage and provide a decision-making basis for subsequent stage-specific seismic retrofitting and optimization of WDNs.

Table 3 Four-Stage seismic resilience indices of WDNs (M_w = 7.5)

	Preparedness (R_b)	Robustness (R_u)	Recoverability (R_a)	Adaptation (R_n)			*RI*
				S1	S2	S3	
Jilin WDN	0.4122	0.6009	0.6181	0.2013	0.0622	0.2785	0.6567
Mianzhu WDN	0.3893	0.6141	0.3688	0.0042	0.0976	0.1396	0.6688

5.2 Decision-Oriented paths for enhancing WDNs resilience

Under the proposed four-stage assessment framework, this study further conducted an in-depth analysis of how the three renovation measures influence the preparedness, robustness, and recoverability of WDNs. Fig. 16 illustrates the resilience levels of the two case WDNs at each stage under different renovation measures when M_w = 7.5. The main findings are summarized as follows:

https://doi.org/10.5194/egusphere-2025-5830
Preprint. Discussion started: 14 January 2026

(1) The resilience enhancement effects of different renovation measures vary considerably among different WDNs. Overall, Renovation Measure S3 exhibits the best performance in enhancing the preparedness, robustness, and recoverability of both WDNs, with total improvement rates of 0.677 and 0.459, respectively. Specifically, for the Jilin WDN, the single pipeline ductility enhancement strategy (S1) yields greater improvements in the preparedness and robustness stages than the network expansion strategy (S2); whereas for the Mianzhu WDN, the network expansion strategy (S2) produces a more pronounced improvement in the preparedness stage (0.251). Therefore, the Jilin WDN is more suitable for adopting the pipeline ductility enhancement strategy (S1), whereas the Mianzhu WDN achieves more pronounced seismic resilience improvements under the network expansion strategy (S2).

(2) Different renovation measures exert varying influences on resilience enhancement across the four stages. For the Jilin WDN (Fig. 16(a)), under the S3 strategy, the improvements in preparedness and robustness reach 0.185 and 0.438, respectively, whereas the enhancement in recoverability is only 0.054. For the Mianzhu WDN (Fig. 16(b)), under the S2 strategy, the preparedness improvement reaches 0.251, which is markedly higher than the 0.002 obtained under the S1 strategy; and at the robustness and recoverability stages, the corresponding improvement values under the S3 strategy are 0.050 and 0.159, respectively.

Therefore, adopting differentiated renovation strategies tailored to the specific characteristics of each WDN is essential for optimizing seismic resilience. For the Jilin WDN, simultaneous implementation of the network expansion and ductility enhancement strategies (S3) can substantially enhance its robustness, whereas for the Mianzhu WDN, prioritizing the network expansion strategy (S2) can maximize the improvement in preparedness. These findings provide a scientific foundation and practical decision support for the seismic optimization and design of WDNs.

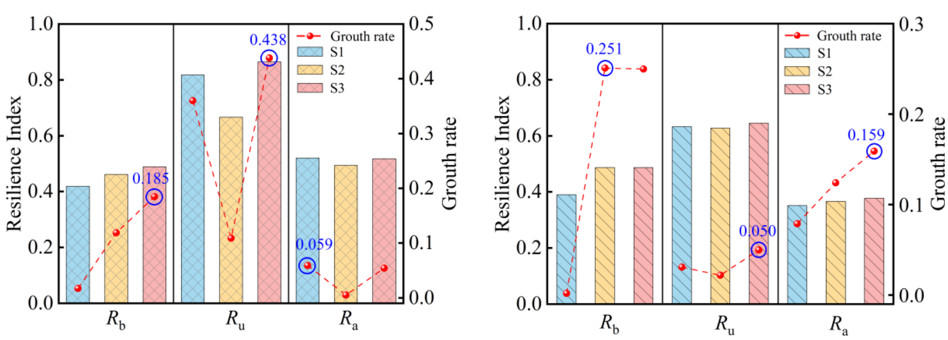

(a) The Jilin WDN

(b) The Mianzhu WDN

Fig. 16 The effect of four-stage resilience retrofit of Water Distribution Networks

6 Conclusion

In this study, a four-stage seismic resilience assessment framework for water distribution networks (WDNs) is developed from a temporal perspective. The framework enables quantitative analysis of both the

https://doi.org/10.5194/egusphere-2025-5830
Preprint. Discussion started: 14 January 2026

inherent disaster-response capacity of WDNs and their post-disaster learning and adaptation, while revealing variations in the four resilience characteristics across different systems. Based on this framework, evaluation indices for each stage were established by considering key attributes of WDNs, including topological structure, energy reserves, pipeline resistance, hydraulic service performance, and recovery duration. The proposed framework was then applied to two case studies—the Jilin and Mianzhu WDNs—to evaluate their seismic resilience across the four stages. From this perspective, the study examined whether these systems possess sufficient resilience and explored the effects of various seismic retrofitting measures on WDN resilience at each stage, thereby providing socio-technical insights for the seismic optimization and design of WDNs. Four-stage resilience assessment indicates that the seismic resilience of WDNs originates from the synergistic evolution of multiple indicators and the dynamic coupling among different stages. The key controlling factors at each stage are both independent and interrelated, suggesting that overall resilience essentially emerges as a dynamic equilibrium among multiple interacting indicators. The main research results are as follows:

(1) Under the four-stage seismic resilience assessment framework proposed in this study, the full process of "pre-disaster preparedness – in-disaster robustness – post-disaster recoverability – long-term adaptation" is integrated into a unified quantitative system for the first time. This framework effectively differentiates resilience variations among WDNs that cannot be captured by traditional assessment methods, rendering the evaluation more comprehensive and precise. It facilitates quantitative analysis of the four-stage resilience characteristics of WDNs, enabling systematic evaluation of the networks' preparedness, robustness, recoverability, and adaptation. In particular, the adaptation assessment establishes a foundation for enhancing the resilience of WDNs.

(2) Case studies indicate that different WDNs display distinct behaviors across the four resilience characteristics; an advantage in one characteristic does not necessarily imply superiority in others. The Mianzhu WDN exhibits an advantage in robustness, whereas the Jilin WDN markedly outperforms in preparedness, recoverability, and adaptation. The stage-specific limitations identified by the framework provide explicit targets for differentiated retrofitting interventions.

(3) Different seismic retrofitting measures exert distinct effects on enhancing resilience at each stage. The pipeline ductility enhancement strategy (S1) produces the most pronounced improvement in the robustness of the Jilin WDN; the network expansion strategy (S2) is the most effective in enhancing the preparedness of the Mianzhu WDN; and the combined retrofitting measure (S3) achieves the maximum overall benefit across all stages.

CRediT authorship contribution statement

Huiquan Miao: Writing – review & editing, Validation, Supervision, Resources, Methodology, Funding acquisition, Conceptualization.

Ya'nan Liu: Writing – review & editing, Writing – original draft, Validation, Methodology,

https://doi.org/10.5194/egusphere-2025-5830
Preprint. Discussion started: 14 January 2026

Investigation, Formal analysis.
Benwei Hou: Validation, Supervision, Resources, Methodology, Conceptualization.
Jie Wei: Validation, Resources, Methodology.
Chengshun Xu: Writing – review & editing, Validation, Supervision, Resources, Project administration, Methodology, Investigation, Funding acquisition, Conceptualization.

Declaration of Competing Interest

The authors declare that they have no known competing financial interests or personal relationships that could have appeared to influence the work reported in this paper.

Acknowledgment

This work is supported by the National Natural Science Foundation of China (Grant No. 52478481, 52494962, 52494963) and the State Key Laboratory of Disaster Reduction in Civil Engineering (Grant No. SLDRCE25-F-29).

References

American Lifelines Alliance (ALA). Seismic guidelines for water pipelines. FEMA, Washington DC, 2005.

Agathokleous, A., Christodoulou, C., Christodoulou, S.E. Topological robustness and vulnerability assessment of water distribution networks. Water Resour. Manage., 31, 4007–4021, https://doi.org/10.1007/s11269-017-1721-7, 2017.

Assad, A., Moselhi, O., Zayed, T. A new metric for assessing resilience of water distribution networks. Water, 11, 1701, https://doi.org/10.3390/w11081701, 2019.

Bata, M.H., Carriveau, R., Ting, D.S.K. Urban water supply systems' resilience under earthquake scenario. Sci. Rep., 12, 20555, https://doi.org/10.1038/s41598-022-23126-8, 2022.

Bouziou, D., O'Rourke, T.D. Response of the Christchurch water distribution system to the 22 February 2011 earthquake. Soil Dyn. Earthq. Eng., 97, 14–24, https://doi.org/10.1016/j.soildyn.2017.01.035, 2017.

Bruneau, M., Chang, S.E., Eguchi, R.T., Lee, G.C., O'Rourke, T.D., Reinhorn, A.M., Shinozuka, M., Tierney, K., Wallace, W.A., Winterfeldt, D.V. A framework to quantitatively assess and enhance the seismic resilience of communities. Earthq. Spectra, 19, 733–752, https://doi.org/10.1193/1.1623497, 2003.

Caetano, J., Ferreira, B., Carrico, N., Covas, D. Redundancy-driven resilience in optimal design of water distribution networks. J. Water Resour. Plann. Manag., 151, 04025037, https://doi.org/10.1061/JWRMD5.WRENG-6613, 2025.

Chen, B., Li, H., Sun, G. Seismic resilience assessment method and multi-objective optimal recovery strategy for large-scale urban water distribution networks. Int. J. Disaster Risk Reduct., 127, 105689, https://doi.org/10.1016/j.ijdrr.2025.105689, 2025.

Cimellaro, G.P., Tinebra, A., Renschler, C., Fragiadaks, M. New resilience index for urban water distribution

https://doi.org/10.5194/egusphere-2025-5830
Preprint. Discussion started: 14 January 2026

networks. J. Struct. Eng., 142, C4015014, https://doi.org/10.1061/(ASCE)ST.1943-541X.0001403, 2016.

Cimellaro, G.P., Villa, O., Bruneau, M. Resilience-based design of natural gas distribution networks. J. Infrastruct. Syst., 21, 05014005, https://doi.org/10.1061/(ASCE)IS.1943-555X.0000204, 2015.

Creaco, E., Franchini, M., Todini, E. The combined use of resilience and loop diameter uniformity as a good indirect measure of network reliability. Urban Water J., 13, 167–181, https://doi.org/10.1080/1573062X.2014.949799, 2014.

Diao, K., Sweetapple, C., Farmani, R., Fu, G., Ward, S., Butler, D. Global resilience analysis of water distribution systems. Water Res., 106, 383–393, https://doi.org/10.1016/j.watres.2016.10.011, 2016.

Eidinger, J.M., Tang, A.K., Davis, C.A. Lushan, Sichuan Province, China, earthquake of 2013: lifeline performance. ASCE, Reston, VA, https://doi.org/10.1061/9780784413661, 2014a.

Fang, Z., Li, X., Li, K. Modeling complexity in engineered infrastructure system: water distribution network as an example. Chaos, 27, 023105, https://doi.org/10.1063/1.4975762, 2017.

Farahmandfar, Z., Piratla, K.R., Andrus, R.D. Resilience evaluation of water supply networks against seismic hazards. J. Pipeline Syst. Eng. Pract., 8, 04016014, https://doi.org/10.1061/(ASCE)PS.1949-1204.0000251, 2016.

Farahmandfar, Z., Piratla, K.R. Comparative evaluation of topological and flow-based seismic resilience metrics for rehabilitation of water pipeline systems. J. Pipeline Syst. Eng. Pract., 9, 04018001, https://doi.org/10.1061/(ASCE)PS.1949-1204.0000293, 2018.

Han, Z., Ma, D., Hou, B., Wang, W. Seismic resilience enhancement of urban water distribution system using restoration priority of pipeline damages. Sustainability, 12, 914, https://doi.org/10.3390/su12030914, 2020.

Hwang, H., Lansey, K. Water distribution system classification using system characteristics and graph-theory metrics. J. Water Resour. Plann. Manag., 143, 4017071, https://doi.org/10.1061/(ASCE)WR.1943-5452.0000850, 2017.

Huang, Y., Luo, B., Zhou, Q., Wang, Q., Zhao, Z. Novel surrogate measures for improving water distribution systems' resilience via pipeline diameter uniformity enhancement. Water Resour. Res., 61, https://doi.org/10.1029/2024WR038237, 2025.

Isoyama, R., Ishida, E., Shirozu, T. Seismic damage estimation procedure for water supply pipelines. Water Supply, 18, 63–68, 2000.

Jayaram, N., Baker, J.W. Efficient sampling and data reduction techniques for probabilistic seismic lifeline risk assessment. Earthq. Eng. Struct. Dyn., 39, 1109–1131, https://doi.org/10.1002/eqe.988, 2010.

Keim, M.E. Building human resilience: the role of public health preparedness and response as an adaptation to climate change. Am. J. Prev. Med., 35, 508–516, https://doi.org/10.1016/j.amepre.2008.08.022, 2008.

Kuraoka, S., Rainer, J.H. Damage to water distribution system caused by the 1995 Hyogo-ken Nanbu earthquake. Can. J. Civ. Eng., 23, 665–677, https://doi.org/10.1139/l96-872, 1996.

Leštáková, M., Logan, K.T., Rehm, I.S., Pelz, P.F., Friesen, J. Do resilience metrics of water distribution systems really assess resilience? A critical review. Water Res., 248, 120820, https://doi.org/10.1016/j.watres.2023.120820, 2024.

Liu, H., Housner, G.W., Xie, L., He, D. The great Tangshan earthquake of 1976. California Institute of Technology, Earthquake Engineering Research Laboratory, https://doi.org/10.7907/AFEE-X539, 2002.

Liu, H., Shuang, Q., Porse, E. Review of the quantitative resilience methods in water distribution networks. Water, 11, 1189, https://doi.org/10.3390/w11061189, 2019.

Liu, S., Zheng, X. Investigation Report on Seismic Damage and Emergency Response of Urban Water Supply Systems in the Wenchuan Earthquake (in Chinese). Tongji University Press, Shanghai, 2013.

https://doi.org/10.5194/egusphere-2025-5830
Preprint. Discussion started: 14 January 2026

Liu, S., Lee, S., Judi, D.R., Parvania, M., Goharian, E., McPherson, T., Burian, S.J. A systematic review of quantitative resilience measures for water infrastructure systems. Water, 10, 164, https://doi.org/10.3390/w10020164, 2018.

Liu, W., Song, Z., Ouyang, M., Li, J. Recovery-based seismic resilience enhancement strategies of water distribution networks. Reliab. Eng. Syst. Saf., 203, 107101, https://doi.org/10.1016/j.ress.2020.107088, 2020.

Long, L., Pan, Z., Yang, H., Yang, Y., Liu, F. A multi-objective method for enhancing the seismic resilience of urban water distribution networks. Symmetry, 17, 1105, https://doi.org/10.3390/sym17071105, 2025.

McGuire, R.K. Probabilistic seismic hazard analysis: early history. Earthq. Eng. Struct. Dyn., 37, 329–338, https://doi.org/10.1002/eqe.765, 2008.

Meng, F., Fu, G., Farmani, R., Sweetapple, C., Butler, D. Topological attributes of network resilience: a study in water distribution systems. Water Res., 143, 306–316, https://doi.org/10.1016/j.watres.2018.06.048, 2018.

Miao, H., Wang, N., Wang, Y., Lin, P. An urban resilience measurement system based on decomposing post-disaster recovery process (in Chinese). J. Nat. Hazards, 30, 10–27, https://doi.org/10.13577/j.jnd.2021.0102, 2021.

Nan, C., Sansavini, G. A quantitative method for assessing resilience of interdependent infrastructures. Reliab. Eng. Syst. Saf., 157, 35–53, https://doi.org/10.1016/j.ress.2016.08.013, 2017.

Ouyang, M., Dueñas-Osorio, L., Min, X. A three-stage resilience analysis framework for urban infrastructure systems. Struct. Saf., 36–37, 23–31, https://doi.org/10.1016/j.strusafe.2011.12.004, 2012.

Pei, S., Zhai, C., Hu, J., Song, Z. Two-stage resilience evaluation for healthcare networks from the adaptation and recoverability perspective. Nat. Hazards Rev., 26, 02025002, https://doi.org/10.1016/j.ijdrr.2023.104019, 2025.

Porse, E., Lund, J. Network analysis and visualizations of water resources infrastructure in California: linking connectivity and resilience. J. Water Resour. Plann. Manag., 142, 4015041, https://doi.org/10.1061/(ASCE)WR.1943-5452.0000556, 2016.

Prasad, T.D., Park, N.S. Multiobjective genetic algorithms for design of water distribution networks. J. Water Resour. Plan. Manag., 130, 73–82, https://doi.org/10.1061/(ASCE)0733-9496(2004)130:1(73), 2004.

Ravadanegh, S.N., Jamali, S., Vaniar, A.M. Multi-infrastructure energy systems resiliency assessment in the presence of multi-hazard disasters. Sustain. Cities Soc., 79, 103687, https://doi.org/10.1016/j.scs.2022.103687, 2022.

RISN-TG041-2022. Guidelines for seismic resilience assessment of urban engineering systems (in Chinese). China Architecture & Building Press, Beijing, 2022.

Sakai, H. Review of research on performance indicators for water utilities. Aqua—Water Infrastruct. Ecosyst. Soc., 73, 167–182, https://doi.org/10.2166/aqua.2024.224, 2024.

Scawthorn, C., O'Rourke, T.D., Blackburn, F.T. The 1906 San Francisco earthquake and fire—enduring lessons for fire protection and water supply. Earthq. Spectra, 22, 135–158, https://doi.org/10.1193/1.2194520, 2006.

Selicato, L., Pagano, A., Esposito, F., Icardi, M. Topological data analysis for resilience assessment of water distribution networks. Math. Comput. Simul., 231, 62–70, https://doi.org/10.1016/j.matcom.2024.12.001, 2025.

Shin, S., Lee, S., Judi, D.R., Parvania, M., Goharian, E., McPherson, T., Burian, S.J. A systematic review of quantitative resilience measures for water infrastructure systems. Water, 10, 164, https://doi.org/10.3390/w10020164, 2018.

Song, Z., Liu, W., Shu, S. Resilience-based post-disaster recovery optimization of water distribution networks.

https://doi.org/10.5194/egusphere-2025-5830
Preprint. Discussion started: 14 January 2026

Int. J. Disaster Risk Reduct., 74, 102934, https://doi.org/10.1016/j.ijdrr.2022.102934, 2022.

Sun, L., Didier, M., Dele, E., Stojadinoic, B. Probabilistic demand and supply resilience model for electric power supply system under seismic hazard. University of British Columbia, Vancouver, https://dx.doi.org/10.14288/1.0076148, 2015.

Sun, L., Stojadinovic, B., Sansavini, G. Agent-based recovery model for seismic resilience evaluation of electrified communities. Risk Anal., 39, 2540–2559, https://doi.org/10.1111/risa.13277, 2019.

Shuang, Q., Liu, H., Porse, E. Review of the quantitative resilience methods in water distribution networks. Water, 11, 1189, https://doi.org/10.3390/w11061189, 2019.

Takada, S., Hassani, N. Lifeline earthquake engineering. University of Tokyo Press, Tokyo, 1992.

Tang, A.K., Eidinger, J.M. Chile earthquake of 2010: lifeline performance. ASCE, Reston, VA, https://doi.org/10.1061/9780784412824, 2013.

Tang, A.K. Wenchuan, Sichuan Province, China, earthquake of 2008: lifeline performance. ASCE, Reston, VA, https://doi.org/10.1061/9780784413333, 2014b.

Todini, E. Looped water distribution networks design using a resilience index based heuristic approach. Urban Water, 2, 115–122, https://doi.org/10.1016/S1462-0758(00)00049-2, 2000.

Torres, J.M., Dueñas-Osorio, L., Li, Q., Yazdani, A. Exploring topological effects on water distribution system performance using graph theory and statistical models. J. Water Resour. Plann. Manag., 143, 04016068, https://doi.org/10.1061/(ASCE)WR.1943-5452.0000709, 2017.

Toro, G.R., Abrahamson, N.A., Schneider, J.F. Model of strong ground motions from earthquakes in central and eastern North America: best estimates and uncertainties. Seismol. Res. Lett., 68, 41–57, https://doi.org/10.1785/gssrl.68.1.41, 1997.

Woolf, S., Twigg, J., Parvania, M., Goharian, E., McPherson, T., Burian, S.J. Towards measurable resilience: A novel framework tool for the assessment of resilience levels in slums. Int. J. Disaster Risk Reduct., 19, 280–302, https://doi.org/10.1016/j.ijdrr.2016.08.003, 2016.

Xu, Z., Chopra, S.S. Network-based assessment of metro infrastructure with a spatial–temporal resilience cycle framework. Reliab. Eng. Syst. Saf., 223, 108434, https://doi.org/10.1016/j.ress.2022.108434, 2022.

Yazdani, A., Jeffrey, P. Water distribution system vulnerability analysis using weighted and directed network models. Water Resour. Res., 48, W06517, https://doi.org/10.1029/2012WR011897, 2012.

Yazdani, A., Otoo, R.A., Jeffrey, P. Resilience enhancing expansion strategies for water distribution systems: a network theory approach. Environ. Model. Softw., 26, 1574–1582, https://doi.org/10.1016/j.envsoft.2011.07.016, 2011.

Yu, X., Wu, Y., Meng, F., Zhou, X., Liu, S., Huang, Y., Wu, X. A review of graph and complex network theory in water distribution networks: mathematical foundation, application and prospects. Water Res., 253, 121238, https://doi.org/10.1016/j.watres.2024.121238, 2024.

Zhang, J., Li, Y., Yuan, H., Du, G., Zhang, M. A demand-based three-stage seismic resilience assessment and multi-objective optimization method of community water distribution networks. Reliab. Eng. Syst. Saf., 250, 110279, https://doi.org/10.1016/j.ress.2024.110279, 2024.

Zhang, W., Wang, N., Nicholson, C., Tehrani, M.H. A stage-wise decision framework for transportation network resilience planning. Reliab. Eng. Syst. Saf., 172, 135–145, https://doi.org/10.1016/j.ress.2017.11.024, 2018.

Zhao, X., Chen, Z., Gong, H. Effects comparison of different resilience enhancing strategies for municipal water distribution network: a multidimensional approach. Math Probl. Eng., 438063, https://doi.org/10.1155/2015/438063, 2015.

Zong, C., Ji, K., Wen, R., Bi, X., Ren, Y., Zhang, X. Seismic resilient three-stage enhancement for gas

https://doi.org/10.5194/egusphere-2025-5830
Preprint. Discussion started: 14 January 2026

distribution network using computational optimization algorithms. Soil Dyn. Earthq. Eng., 152, 107057, https://doi.org/10.1016/j.soildyn.2021.107057, 2022.